Electronic Research Archive

https://www.aimspress.com/journal/era

ERA, 33(12): 7528–7550.
DOI: 10.3934/era.2025332
Received: 16 October 2025
Revised: 04 December 2025
Accepted: 09 December 2025
Published: 16 December 2025

Research article

Dynamical analysis of discrete models for mosquito population suppression

Ruibin Jiang, Zhiming Guo* and Ruiqiang Zhuo

School of Mathematics and Information Science, Guangzhou University, Guangzhou 510006, China

* **Correspondence:** Email: guozm@gzhu.edu.cn.

Abstract: Amid the global challenge of mosquito-borne disease transmission, sterile insect technology (SIT) has emerged as a promising biological control strategy. Based on the classical Beverton–Holt model and the assumption of complete cytoplasmic incompatibility (CI), we develop a discrete-time model with overlapping generations and a corresponding integro-difference equation (IDE) to investigate the population dynamics under different release strategies for infected male mosquitoes. For the discrete-time model, we apply stability and bifurcation theory to determine the existence and stability of equilibria and derive the release threshold r^* above which the wild mosquito population is successfully suppressed. Analysis of the IDE model yields a lower release threshold r^{**} and a critical patch-size L^*. Comparison of the two models demonstrates that spatial diffusion reduces the required release threshold for achieving population suppression.

Keywords: stability; bifurcation; integro-difference equation; traveling wave; critical patch-size

1. Introduction

Many highly pathogenic viruses and parasites that trigger infectious diseases such as malaria, dengue fever, yellow fever, filariasis, and chikungunya are transmissible via mosquitoes. In the context of the accelerating pace of globalization, especially the substantial growth in international travel and trade, the geographical distribution of invasive mosquito species has significantly expanded. As a result, the mosquito-borne infectious diseases that ensue present a grave threat to people's health in endemic areas across the globe [1–4]. However, there are still no effective vaccines or specific treatments for most mosquito-borne infectious diseases. Therefore, mosquito vector control remains the main method to limit the spread of mosquito-borne infectious diseases. At present, the integrated vector management (IVM) strategy is advocated for mosquito vector control, which emphasizes the priority of environmental control. At the same time, it is emphasized that the combination of chemical control, biological control, genetic control, and other methods should be applied to reduce the number of mosquito population and control disease transmission [5, 6].

It has been found that the most effective biological control measure at present is the application of SIT to block virus transmission, which mainly involves releasing male mosquitoes infected with *Wolbachia* into the wild. A large number of experiments have shown that *Wolbachia* symbiotic bacteria can inhibit the replication of mosquito-borne disease viruses in mosquitoes, and thereby reduces the probability of virus transmission between humans and mosquitoes to some extent. Since *Wolbachia* is maternally inherited, its offspring will also be infected as long as the female mosquitoes are infected with *Wolbachia*. In addition, *Wolbachia* can induce cytoplasmic incompatibility (CI) in the host, which is manifested in the early embryo death if infected male mosquitoes mate with uninfected female mosquitoes, but the embryo will develop normally in other cases [7, 8]. Based on these characteristics of *Wolbachia*, many scientists in China have carried out mosquito population suppression experiments in the field and achieved a series of remarkable results [9, 10]. Compared with traditional control measures, the application of *Wolbachia* is a new and environmentally friendly control method.

In recent years, many mosquito population suppression models with different releasing strategies have been formulated, such as impulsive differential equation models [11–13], discrete models [14–18], and reaction-diffusion models [19–21]. In 2022, Zhang et al. [11] proposed a switching ordinary differential equation model with an assumption that mosquito-borne infectious diseases exhibit seasonal epidemic pattern. Surprisingly, seasonal switch gives rise to rich dynamics. This includes the existence of either a unique periodic solution or precisely two periodic solutions, which are demonstrated by using the qualitative property of the Poincaré map. In view of four release strategies, early acting bisex (EBS), late acting bisex (LBS), early acting female-killing (EFK), and late acting female-killing (LFK), Yu and Li [22] recently established four discrete models, respectively,

$$EBS : w_{n+1} = \frac{r_0 w_n^2}{\xi_1 w_n^2 + w_n + c},$$

$$LBS : w_{n+1} = \frac{r_0 w_n^2}{\xi_1 w_n^2 + (1 + 2\xi_2 c) w_n + c},$$

$$EFK : w_{n+1} = \frac{w_{n-1} + c}{(w_n + c)(w_{n-1} + c) + \gamma b c w_{n-1}} \frac{r_0 w_n (w_n + c)}{\xi_1 w_n^2 + (1 + \xi_2 c) w_n + c} w_n,$$

and

$$LFK : w_{n+1} = \frac{w_{n-1} + c}{(w_n + c)(w_{n-1} + c) + \gamma b c w_{n-1}} \frac{r_0 w_n (w_n + c)}{\xi_1 w_n^2 + (1 + 2\xi_2 c) w_n + c} w_n,$$

to investigate the existence and stability of positive equilibria and gave a release threshold value of sterile mosquitoes for each model. We found that most authors did not consider spatial factors, which can have a significant impact on mosquito population. To investigate whether diffusion will affect our release threshold value, we not only build a discrete model but also give the corresponding integro-difference equation model for comparison.

The following scalar difference equation with Beverton-Holt-type growth function [23],

$$u_{t+1} = \frac{b u_t}{1 + c u_t}, \tag{1.1}$$

is an autonomous discrete system used to describe the recursive relationship between generation $t + 1$ and t. It was originally proposed in 1957 to model fish stock recruitment. Parameter $b > 0$ measures

the birth rate of fish population. Parameter $c > 0$ is described as the strength of density dependence, which also can be understood as intraspecific competition coefficient.

By assuming that wild mosquito population is overlapping, we present a discrete model for inhibiting the growth of wild mosquito population by releasing infected *Wolbachia* males. Let ω_t be the density of wild mosquito population for generation t, then the model can be expressed as

$$\omega_{t+1} = B(\omega_t, r) + (1 - d)\omega_t, \tag{1.2}$$

where $B(\cdot, r)$ is the mosquito population growth function, r represents the number of released infected males with $r \geq 0$, and d denotes the mortality of mosquito population with $0 < d < 1$.

In order to describe the variation of wild mosquito population more accurately, the growth function that we adopt is the Beverton-Holt function, but it is different from (1.1) because there also exists interspecific competition between wild mosquitoes and infected males. Furthermore, we introduce the following two crucial biological assumptions:

(A1) Wild mosquitoes exhibit a uniform sex distribution (i.e., the ratio of males to females is 1:1).
(A2) Infected males possess the same mating competitiveness as wild male mosquitoes.

Therefore, the probability that wild female mosquitoes at generation t mate with infected males is $\frac{r}{\frac{1}{2}\omega_t + r}$. Besides, as the current experimental data indicate that the infection of a novel *Wolbachia* strain in *Ae. albopictus* in Guangzhou leads to almost complete CI as reported in [24], the birth rate of wild mosquito population becomes $b \cdot \frac{\omega_t}{r+\omega_t}$. By modifying (1.1), a new Beverton-Holt function can be derived as follows:

$$B(\omega_t, r) = \frac{b\omega_t}{1 + c_1 r + c_2\omega_t} \frac{\omega_t}{r + \omega_t}, \tag{1.3}$$

where $b > 0$ represents the birth rate of wild mosquito population, and $c_1 > 0$ and $c_2 > 0$ represent the interspecific competition and intraspecific competition, respectively. Since the difference between interspecific competition and intraspecific competition in mosquito population can be ignored, by setting $c_1 = c_2 = c$, the subsequent model is established:

$$\omega_{t+1} = \frac{b\omega_t}{1 + cr + c\omega_t} \frac{\omega_t}{r + \omega_t} + (1 - d)\omega_t. \tag{1.4}$$

We can reduce the number of parameters by nondimensionalizing the model, letting $\overline{\omega}_t = c\omega_t$ and $R = cr \geq 0$. Substituting these into (1.4) yields

$$\overline{\omega}_{t+1} = \frac{b\overline{\omega}_t}{1 + R + \overline{\omega}_t} \frac{\overline{\omega}_t}{R + \overline{\omega}_t} + (1 - d)\overline{\omega}_t. \tag{1.5}$$

For notational simplicity, the variable is still denoted as ω_t. Thus, we can obtain the following nonspatial model

$$\omega_{t+1} = \frac{b\omega_t}{1 + R + \omega_t} \frac{\omega_t}{R + \omega_t} + (1 - d)\omega_t \triangleq F(\omega_t). \tag{1.6}$$

It should be noted that for any $\omega > 0$, $F'(\omega) = \frac{b\omega[2R(1+R+\omega)+\omega]}{(1+R+\omega)^2(R+\omega)^2} + (1 - d) > 0$, i.e., $F(x)$ is a nonlinear monotonically increasing function with $F(0) = 0$.

Furthermore, a key aspect of the insect life cycle involves many species hatching from eggs, developing through a larval stage, undergoing pupation, and ultimately emerging as adults. These

adults fly, lay eggs to produce the next generation, and then die. One common feature of such life cycle is the separation of the growth phase, during which spatial dispersion is negligible, and the dispersion phase, during which no growth occurs [25]. This holds true for wild mosquitoes. Integro-difference equations (IDEs) are the best tool to describe the life cycle of these insects. In the following, we will establish an IDE incorporating the spatial influence to characterize the dynamic behavior of wild mosquito population. Let $\omega_t(x)$ be the spatial density of wild mosquito population in generation t and at location x, then the IDEs model is given by

$$\omega_{t+1}(x) = \int_{\Omega} K(x, y)F(\omega_t(y))\mathbf{d}y, \tag{1.7}$$

where $K(x, y)$ is a dispersal kernel, $H(\omega)$ is a growth function, and $\Omega \subset \mathbb{R}^N$ is a habitat domain.

An outline of this paper is as follows: We devote Section 2 to a discussion of the nonspatial dynamics, which includes the stability of equilibria and bifurcation behavior, as well as the release threshold value r^* for the success of mosquito suppression. In Section 3, the direction of traveling waves and critical patch-size for Laplace kernel in integro-difference equation are established. Numerical simulations to support our theoretical results for two discrete models are presented in Section 4. Finally, we give some comments about the release threshold value by comparing the nonspatial and spatial models in Section 5.

2. The case of the difference equation model

In this section, we primarily analyze the dynamics of (1.6) for different release levels of infected males. The release threshold value of infected males for successful suppression will be given.

2.1. Positivity and boundedness

Lemma 2.1. *For any initial value $\omega_0 \geq 0$, the solution ω_t of* (1.6) *is nonnegative and satisfies $0 \leq \omega_t \leq \frac{b}{d}$ for each t.*

Proof. Since all the parameters in (1.6) are nonnegative, the solution ω_t must be nonnegative for any initial value $\omega_0 \geq 0$. We now prove the boundedness of the solution ω_t. It follows immediately from (1.6) that $\omega_{t+1} \leq b + (1 - d)\omega_t$ for each t. Letting $d_1 = 1 - d$, we obtain $\omega_{t+1} - d_1\omega_t \leq b$. From this recursive relation, we can get the following inequalities:

$$\begin{cases} \omega_t - d_1\omega_{t-1} \leq b, \\ d_1\omega_{t-1} - d_1^2\omega_{t-2} \leq d_1 b, \\ d_1^2\omega_{t-2} - d_1^3\omega_{t-3} \leq d_1^2 b, \\ ..... \\ d_1^{t-1}\omega_1 - d_1^t\omega_0 \leq d_1^{t-1} b. \end{cases}$$

Adding all inequalities above leads to

$$\omega_t - d_1^t\omega_0 \leq b(1 + d_1 + d_1^2 + \cdots + d_1^{t-1}) = b\frac{1 - d_1^t}{1 - d_1}. \tag{2.1}$$

It is clear from (2.1) that

$$\omega_t \leq \frac{b}{d}(1 - d_1^t) + \frac{b}{d}d_1^t = \frac{b}{d}$$

so long as $\omega_0 \leq \frac{b}{d}$. Consequently, the solution ω_t is bounded, and the positive invariant set of (1.6) is

$$P = \{\omega_t \in \mathbb{R} | 0 \leq \omega_t \leq \frac{b}{d}\}.$$

2.2. Equilibria and stability

A significant component of a general dynamic system that has been used to capture the variation of wild mosquito population is the existence and stability of equilibria. First, we use a lemma to enumerate the nonnegative equilibria of (1.6).

Lemma 2.2. *Let*

$$R^* = \frac{(b-d)^2}{4bd}. \tag{2.2}$$

Then the following statements are true:

(I) If $b \leq d$ and $R \geq 0$, then there exists exactly one equilibrium $\omega_0^* = 0$.

(II) If $b > d$, then $\omega_0^* = 0$ always exists. Additionally, for the positive equilibria of (1.6)*, there exist the following four cases:*

(i) If $R = 0$, then (1.6) *admits exactly one positive equilibrium, denoted as $\omega_1^* = \frac{b}{d} - 1$.*

(ii) If $0 < R < R^*$, then there exist exactly two positive equilibria, denoted as

$$\omega_1^* = -\frac{(2R + 1 - \frac{b}{d}) + \sqrt{\beta(R)}}{2} \quad \text{and} \quad \omega_2^* = \frac{-(2R + 1 - \frac{b}{d}) + \sqrt{\beta(R)}}{2},$$

where $\beta(R) = (2R + 1 - \frac{b}{d})^2 - 4R(R + 1) = -\frac{4b}{d}R + (1 - \frac{b}{d})^2$.

(iii) If $R = R^*$, then there exists exactly one positive equilibrium, denoted as $\omega^* = \frac{b^2-d^2}{4bd}$.

(iv) If $R > R^*$, then (1.6) *has no positive equilibria.*

Proof. First, note that $\omega_0^* = 0$ is an equilibrium of (1.6). To investigate the existence of other positive equilibria, we begin with the equation

$$\frac{b\omega}{(1 + R + \omega)(R + \omega)} = d, \tag{2.3}$$

which is equivalent to

$$\omega^2 + \left(2R + 1 - \frac{b}{d}\right)\omega + R(R + 1) = 0.$$

Let

$$h(\omega, R) = \omega^2 + (2R + 1 - \frac{b}{d})\omega + R(R + 1). \tag{2.4}$$

The positive equilibria of (1.6) are given by the positive roots of $h(\omega, R) = 0$.

(I) If $b \leq d$ and $R \geq 0$, we have $2R+1-\frac{b}{d} \geq 0$. This implies that the axis of symmetry is nonpositive. Therefore, (2.4) has no positive roots.

(II) Suppose that $b > d$.

(i) If $R = 0$, $h(\omega, R) = \omega^2 + (1 - \frac{b}{d})\omega$. Therefore, it is straightforward to know that (2.4) has a positive root $\omega_1^* = \frac{b}{d} - 1$.

(ii) Notice that if $2R + 1 - \frac{b}{d} < 0$, i.e., $R < \frac{b-d}{2d}$, (2.4) may have positive real roots. Consider the discriminant

$$\Delta = (2R + 1 - \frac{b}{d})^2 - 4R(R + 1) = -\frac{4b}{d}R + (1 - \frac{b}{d})^2 \triangleq \beta(R), \tag{2.5}$$

where $\beta(R)$ is a linear function with respect to R. Setting $\beta(R) = 0$, we obtain a critical value $R^* = \frac{(b-d)^2}{4bd} < \frac{b-d}{2d}$. Therefore, $\beta(R) > 0$ for $0 < R < R^*$. In this case, $h(x, R) = 0$ has two positive real roots, denoted by

$$\omega_1^* = -\frac{(2R + 1 - \frac{b}{d}) + \sqrt{\beta(R)}}{2}, \omega_2^* = \frac{-(2R + 1 - \frac{b}{d}) + \sqrt{\beta(R)}}{2},$$

respectively.

(iii) From the above arguments, it can be seen that (2.4) has exactly one positive real root $\omega^* = \frac{b^2-d^2}{4bd}$ if and only if $R^* = \frac{(b-d)^2}{4bd}$.

(iv) At last, if $R^* < R < \frac{b-d}{2d}$, we have $2R + 1 - \frac{b}{d} < 0$ and $\beta(R) < 0$, so (2.4) has no positive real roots. When $R \geq \frac{b-d}{2d}$, the same result also holds. As a consequence, (1.6) has no positive equilibria when $R > R^*$.

Subsequently, we will analyze the stability of each equilibrium in Lemma 2.2 for different value ranges of b, d, and R.

Theorem 2.1. *Suppose that $b \leq d$ and $R \geq 0$, then* (1.6) *exists exactly a globally asymptotically stable equilibrium $\omega_0^* = 0$.*

Proof. Lemma 2.1 implies that there exists an equilibrium $\omega_0^* = 0$ for $b \leq d$ and $R \geq 0$. In this case, it is sufficient to guarantee that

$$\frac{b\omega}{(1 + R + \omega)(R + \omega)} - d < 0.$$

Due to $|F'(0)| = |1 - d| < 1$, we know that the equilibrium $\omega_0^* = 0$ is locally asymptotically stable. Next, we will establish its global stability. Given any initial value $\omega_0 > 0$, we can show that

$$\begin{aligned}\omega_1 - \omega_0^* &= \Big[\frac{b\omega_0^2}{(1 + R + \omega_0)(R + \omega_0)} + (1 - d)\omega_0\Big] - \Big[\frac{b\omega_0^{*2}}{(1 + R + \omega_0^{*2})(R + \omega_0^{*2})} + (1 - d)\omega_0\Big] \\ &= F(\omega_0) - F(\omega_0^*) > 0\end{aligned}$$

by virtue of the fact that $F(\omega)$ is a monotonically increasing function. Thus, when $\omega_0 > 0 = \omega_0^*$, we have $\omega_t > \omega_0^*$. It follows from (1.6) that

$$\frac{\omega_{t+1}}{\omega_t} = 1 + \frac{b\omega_t}{(1 + R + \omega_t)(R + \omega_t)} - d < 1,$$

which means the solution ω_t is monotonically decreasing and converges to ω_0^*. Consequently, $\omega_0^* = 0$ is globally asymptotically stable.

However, it is of interest to study the dynamics of wild mosquito population in different release strategies of infected male mosquitoes. Furthermore, we explore the threshold value above which wild mosquito population can be successfully suppressed. Within the framework of (1.6), we always assume $b > d$.

2.2.1. Case(i): $R = 0$

We consider the first case where $R = 0$, which means that there are no infected male mosquitoes being released. Under these conditions, (1.6) can be simplified to

$$\omega_{t+1} = \frac{b\omega_t}{1+\omega_t} + (1-d)\omega_t, \tag{2.6}$$

i.e., $F(\omega) = \frac{b\omega}{1+\omega} + (1-d)\omega$.

Theorem 2.2. *Assume that $b > d$ and $R = 0$. (1.6) has two equilibria, $\omega_0^* = 0$ and $\omega_1^* = \frac{b}{d} - 1$, in which ω_0^* is unstable and ω_1^* is globally asymptotically stable.*

Proof. If $b > d$ and $R = 0$, then it is immediate from (2.6) that

$$F'(\omega) = \frac{b}{(1+\omega)^2} + 1 - d > 0.$$

Hence, $F(\omega)$ is monotonically increasing. From Lemma 2.2(I)(i), we obtain $|F'(\omega_0^*)| = |1 + b - d| > 1$ and $|F'(\omega_1^*)| = |\frac{d^2}{b} + 1 - d| < 1$ when $b > d$. As a consequence, $\omega_0^* = 0$ is unstable, and $\omega_1^* = \frac{b}{d} - 1$ is locally asymptotically stable. Proceeding as in the proof of Theorem 2.1, given any initial value $\omega_0 > 0$ satisfying $\omega_0 > \omega_1^*$, we can obtain

$$\omega_1 - \omega_1^* = F(\omega_0) - F(\omega_1^*) > 0.$$

So, we have $\omega_t > \omega_1^*$ for each $t > 1$. Furthermore, it follows from (2.6) that

$$\frac{\omega_{t+1}}{\omega_t} = \frac{b}{1+\omega_t} + 1 - d < \frac{b}{1+\omega_1^*} + 1 - d = 1,$$

which implies that ω_t is monotonically decreasing and converges to ω_1^*. A completely analogous argument can be made when the initial value meets $0 < \omega_0 < \omega_1^*$. So, the dynamics of (1.6) are the same as Beverton-Holt model (1.1), where ω_0^* is always unstable and ω_1^* is globally asymptotically stable.

2.2.2. Case(ii): $0 < R < R^*$

For $R > 0$, *Wolbachia*-infected mosquitoes invade wild mosquito population, inducing complex dynamics in wild population. In this case, $\omega_0^* = 0$ is always an asymptotically stable equilibrium for (1.6) since $|F'(0)| = |1 - d| < 1$.

Theorem 2.3. *Assume that $b > d$ and $0 < R < R^*$. Then it has three nonnegative equilibria, $\omega_0^* = 0$, $\omega_1^* = -\frac{(2R+1-\frac{b}{d})+\sqrt{\beta(R)}}{2}$, and $\omega_2^* = \frac{-(2R+1-\frac{b}{d})+\sqrt{\beta(R)}}{2}$, in which ω_0^* and ω_2^* are locally asymptotically stable and ω_1^* is always unstable.*

Proof. Throughout the proof, we always assume that ω is an equilibrium of (1.6). Note that

$$F'(\omega) = \frac{b\omega[2R(1+R+\omega)+\omega]}{(1+R+\omega)^2(R+\omega)^2} + (1-d), \tag{2.7}$$

and its positive equilibria satisfy (2.3). Then, in combination with (2.7), we get

$$\begin{aligned} F'(\omega) &= d\frac{2R(1+R+\omega)+\omega}{(1+R+\omega)(R+\omega)} + (1-d) \\ &= d\Big(\frac{2R}{R+\omega} + \frac{d}{b}\Big) + (1-d) \\ &= 1 + d\Big(\frac{2R}{R+\omega} + \frac{d}{b} - 1\Big). \end{aligned} \tag{2.8}$$

According to the difference equation theory, if $|F'(\omega)| < 1$ holds, or equivalently,

$$-\frac{2}{d} < \frac{2R}{R+\omega} + \frac{d}{b} - 1 < 0, \tag{2.9}$$

then ω is locally asymptotically stable. However, if the converse holds, ω is unstable for

$$\frac{2R}{R+\omega} + \frac{d}{b} - 1 < -\frac{2}{d} \text{ or } \frac{2R}{R+\omega} + \frac{d}{b} - 1 > 0. \tag{2.10}$$

Denote $a = \frac{b}{d}$, and it is evident that $a > 1$. We are also aware of, by Lemma 2.2(II)(ii), that (1.6) admits two positive equilibria

$$\omega_1^* = -\frac{(2R+1-a) + \sqrt{\beta(R)}}{2}, \ \omega_2^* = \frac{-(2R+1-a) + \sqrt{\beta(R)}}{2}.$$

Besides, we can rewrite (2.5) as $\beta(R) = -4aR + (1-a)^2$ with the range of $\sqrt{\beta(R)} \in (0, a-1)$ if $0 < R < R^*$.

Substituting ω_1^* into inequality (2.10) yields

$$\begin{aligned} \frac{2R}{R+\omega} + \frac{1}{a} - 1 &= \frac{2R}{R+\omega_1^*} + \frac{1}{a} - 1 \\ &= \frac{1}{a} - 1 - \frac{4R}{1-a+\sqrt{\beta(R)}} \\ &= \frac{(1-a)(1-a+\sqrt{\beta(R)}) - 4Ra}{a(1-a+\sqrt{\beta(R)})} \\ &= \frac{1}{a}\sqrt{\beta(R)} > 0. \end{aligned}$$

Hence, ω_1^* is unstable. As for the positive equilibrium ω_2^*, a similar calculation can be made to show that

$$\begin{aligned} \frac{2R}{R+\omega} + \frac{1}{a} - 1 &= \frac{2R}{R+\omega_2^*} + \frac{1}{a} - 1 \\ &= \frac{2R}{R + \frac{-(2R+1-a)+\sqrt{\beta(R)}}{2}} + \frac{1}{a} - 1 \\ &= \frac{-\beta(R) - (a-1)\sqrt{\beta(R)}}{a(a-1+\sqrt{\beta(R)})} < 0. \end{aligned}$$

Besides, if

$$\frac{-\beta(R)-(a-1)\sqrt{\beta(R)}}{a(a-1+\sqrt{\beta(R)})}>-\frac{2}{d},$$

or alternatively,

$$\beta(R)+(a-1-\frac{2a}{d})\sqrt{\beta(R)}-\frac{2a(a-1)}{d}<0,$$

then ω_2^* is locally asymptotically stable. We define $f(\sqrt{\beta})=\beta+(a-1-\frac{2a}{d})\sqrt{\beta}-\frac{2a(a-1)}{d}$, $\sqrt{\beta(R)}\in(0,a-1)$. Since $f(0)=-\frac{2a(a-1)}{d}<0$, $f(a-1)=2(a-1)(a-1-\frac{2a}{d})<0$, the inequality $f(\sqrt{\beta})<0$ holds for any given $\sqrt{\beta}\in(0,a-1)$. Therefore, ω_2^* is locally asymptotically stable. The proof is complete.

2.2.3. Case(iii): $R=R^*$

We now shift our focus to the mathematical problem in the scenario where $R=R^*=\frac{(b-d)^2}{4bd}$.

Theorem 2.4. *Assume that $b>d$ and $R=R^*$. Then* (1.6) *admits a locally asymptotically stable trivial point $\omega_0^*=0$ and a semi-stable positive equilibrium $\omega^*=\frac{b^2-d^2}{4bd}$.*

Proof. From the previous analysis, we can deduce that the trivial point $\omega_0^*=0$ is locally asymptotically stable. The remaining claim in Theorem 2.4 can be verified in the same manner as demonstrated previously. First, according to Lemma 2.2(II)(iii), we have $h(\omega,R^*)>0$, that is,

$$\frac{b\omega}{(1+R^*+\omega)(R^*+\omega)}-d<0 \tag{2.11}$$

when $\omega\in(0,\omega^*)\cup(\omega^*,+\infty)$. Given any initial value $\omega_0>\omega^*$, it is easy to see that

$$\omega_1-\omega^*=F(\omega_0)-F(\omega^*)>0.$$

By iterating, we can conclude that $\omega_t>\omega^*$ for each $t\geq 1$. Using (1.6) and (2.11), we arrive at

$$\frac{\omega_{t+1}}{\omega_t}=1+\frac{b\omega_t}{(1+R^*+\omega_t)(R^*+\omega_t)}-d<1,$$

which indicates that the solution ω_t is monotonically decreasing and

$$\lim_{t\to+\infty}\omega_t=\omega^*.$$

Hence, $\omega^*=\frac{b^2-d^2}{4bd}$ is semi-stable, as asserted.

2.2.4. Case(iv): $R>R^*$

If the number of released infected males is greater than R^*, we can obtain the following result.

Theorem 2.5. *Suppose that $b>d$ and $R>R^*$, then the trivial equilibrium $\omega_0^*=0$ is globally asymptotically stable.*

Proof. The proof is trivial, and we omit it here.

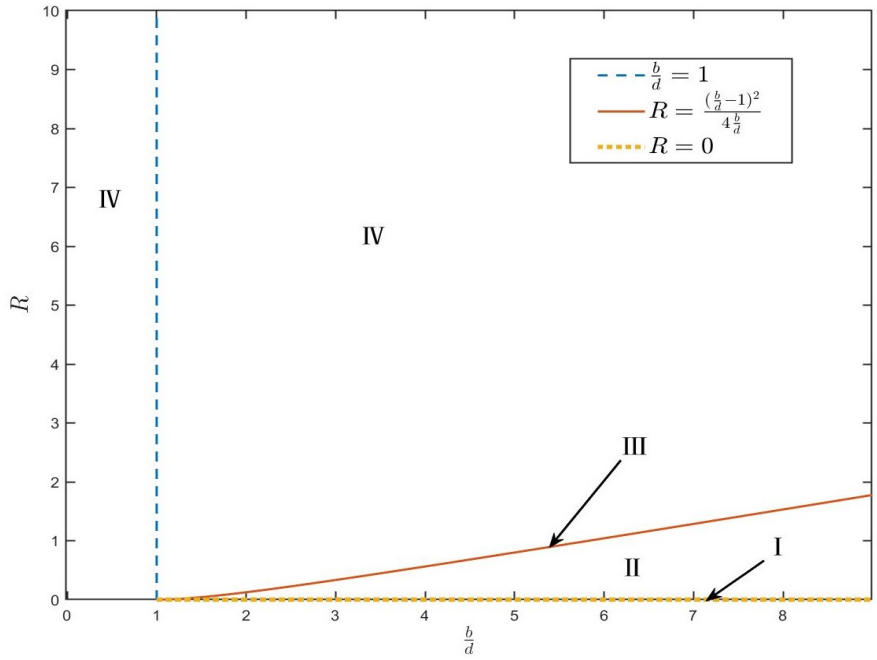

Figure 1. The value range of each parameter in four different cases.

To summarize this part comprehensively, the parameter ranges in four different cases can be more effectively presented as depicted in Figure 1, where straight line I and III correspond to Case(i) and Case(iii), respectively, while region II and IV represent Case(ii) and Case(iv).

2.3. Saddle node bifurcation

Recall that

$$F(\omega,R)=\frac{b\omega}{1+R+\omega}\frac{\omega}{R+\omega}+(1-d)\omega=b\left(1+\frac{R^2}{\omega+R}-\frac{(R+1)^2}{\omega+R+1}\right)+(1-d)\omega.$$

According to the equilibrium equation (2.3), by differentiating $F(\omega,R)$ with respect to ω and R, we get the desired equations

$$\begin{aligned}\frac{\partial^2F(\omega,R)}{\partial\omega^2}&=\frac{2b}{(R+\omega)(R+\omega+1)}-\frac{4b\omega}{(R+\omega)(R+\omega+1)^2}-\frac{4b\omega}{(R+\omega)^2(R+\omega+1)}\\&\quad+\frac{2b\omega^2}{(R+\omega)(R+\omega+1)^3}+\frac{2b\omega^2}{(R+\omega)^2(R+\omega+1)^2}+\frac{2b\omega^2}{(R+\omega)^3(R+\omega+1)}\\&=\frac{2d}{\omega}+\frac{2d^2}{b}+2d\omega\Big(\frac{1}{(R+\omega+1)^2}+\frac{1}{(R+\omega)^2}\Big)-4d\Big(\frac{1}{R+\omega+1}+\frac{1}{R+\omega}\Big)\end{aligned}\tag{2.12}$$

and

$$\begin{aligned}\frac{\partial F(\omega,R)}{\partial R} &= -\frac{b\omega^2(R+\omega+R+\omega+1)}{(R+\omega)^2(R+\omega+1)^2}\\ &= -\frac{b\omega^2}{(R+\omega)(R+\omega+1)^2} - \frac{b\omega^2}{(R+\omega)^2(R+\omega+1)}\\ &= -d\omega\Big(\frac{1}{R+\omega+1}+\frac{1}{R+\omega}\Big).\end{aligned} \tag{2.13}$$

Combining Lemma 2.2(II)(iii) and Eqs (2.8), (2.12), and (2.13), we see that $F(\omega^*,R^*)=0$,

$$\begin{aligned}\frac{\partial F(\omega^*,R^*)}{\partial \omega} &= 1+d\Big(\frac{2R^*}{R^*+\omega^*}+\frac{d}{b}-1\Big)\\ &= 1+d\Big(\frac{2\frac{(b-d)^2}{4bd}}{\frac{(b-d)^2}{4bd}+\frac{b^2-d^2}{4bd}}+\frac{d}{b}-1\Big)\\ &= 1+d\Big(\frac{2(b-d)^2}{(b-d)^2+b^2-d^2}+\frac{d}{b}-1\Big)\\ &= 1,\end{aligned}$$

$$\begin{aligned}\frac{\partial^2 F(\omega^*,R^*)}{\partial \omega^2} &= \frac{2d}{\omega^*}+\frac{2d^2}{b}+2d\omega^*\Big(\frac{1}{(R^*+\omega^*+1)^2}+\frac{1}{(R^*+\omega^*)^2}\Big)-4d\Big(\frac{1}{R^*+\omega^*+1}+\frac{1}{R^*+\omega^*}\Big)\\ &= \frac{2d}{\frac{b^2-d^2}{4bd}}+\frac{2d^2}{b}+2d\frac{b^2-d^2}{4bd}\Big(\frac{1}{(\frac{(b-d)^2}{4bd}+\frac{b^2-d^2}{4bd}+1)^2}+\frac{1}{(\frac{(b-d)^2}{4bd}+\frac{b^2-d^2}{4bd})^2}\Big)\\ &\quad -4d\Big(\frac{1}{\frac{(b-d)^2}{4bd}+\frac{b^2-d^2}{4bd}+1}+\frac{1}{\frac{(b-d)^2}{4bd}+\frac{b^2-d^2}{4bd}}\Big)\\ &= \frac{8bd^2}{b^2-d^2}+\frac{2d^2}{b}+\frac{2d^2}{b}\Big(\frac{b-d}{b+d}+\frac{b+d}{b-d}\Big)-\frac{16bd^2}{b^2-d^2}\\ &= \frac{2d^2}{b}\Big(1+\frac{2(b^2+d^2)}{b^2-d^2}\Big)-\frac{8bd^2}{b^2-d^2}\\ &= \frac{2d^2(3b^2+d^2)}{b(b^2-d^2)}-\frac{8bd^2}{b^2-d^2}\\ &= -\frac{2d^2(b^2-d^2)}{b(b^2-d^2)}=-\frac{2d^2}{b}<0,\\ \frac{\partial F(\omega^*,R^*)}{\partial R} &= -d\omega^*\Big(\frac{1}{R^*+\omega^*+1}+\frac{1}{R^*+\omega^*}\Big)\\ &= -d\frac{b^2-d^2}{4bd}\Big(\frac{1}{\frac{(b-d)^2}{4bd}+\frac{b^2-d^2}{4bd}+1}+\frac{1}{\frac{(b-d)^2}{4bd}+\frac{b^2-d^2}{4bd}}\Big)\\ &= -d\frac{b^2-d^2}{4bd}\Big(\frac{2d}{b+d}+\frac{2d}{b-d}\Big)\\ &= -d<0,\end{aligned}$$

which imply that (1.6) will undergo a saddle-node bifurcation at the positive equilibrium (ω^*,R^*). It means there exists $\delta>0$ such that (1.6) has two equilibria, ω_1^* and ω_2^*, in the neighborhood of $\omega=\omega^*$

when $-\delta + R^* < R < R^*$, where $\omega_1^* < \omega^*$ is unstable and $\omega_2{}^* > \omega^*$ is locally asymptotically stable. Otherwise, (1.6) has no equilibrium in the neighborhood of $\omega = \omega^*$ when $R^* < R < R^* + \delta$. The result of this bifurcation for $b = 4$ and $d = 0.2$ is presented in Figure 2, where the solid line indicates stability and dashed line indicates instability.

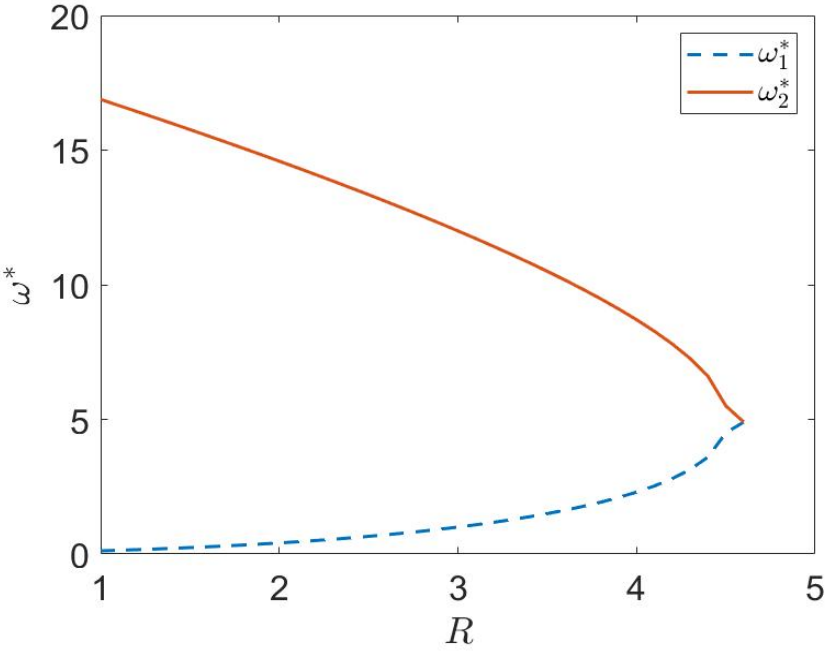

Figure 2. The schematic diagram of saddle-node bifurcation for Model (1.6).

3. The case of the IDE model

In Section 2, we explicitly calculated the release threshold of infected males for a difference equation model with a monotonically increasing growth function. However, our previous analysis overlooked the influence of spatial factors on population dynamics. To address this gap, we use the framework of IDEs to simulate the mosquito population suppression. In the following work, we consider the IDE model corresponding to Case(ii). That is, (1.7) can be converted into

$$\omega_{t+1}(x) = \int_{\Omega} K(x, y) F(\omega_t(y)) \mathbf{d}y, \tag{3.1}$$

where F is defined in (1.6) and $b > d$, $0 < R < R^*$. Up to now, most studies have assumed that the dispersal kernel depends only on the distance of movement. In this case, $K(x, y)$ is assumed to be $\widetilde{K}(|x - y|)$ describing the distribution of dispersal distances. It is implicitly assumed that dispersal is isotropic, meaning it is the same in all directions. There are several assumptions regarding the kernel function:

(i) $\widetilde{K}(x) \geq 0$. *If* $B_1 = \inf\{x : \widetilde{K}(x) > 0\}$, $B_2 = \sup\{x : \widetilde{K}(x) > 0\}$, *then* $\widetilde{K}(x) > 0$ *in* (B_1, B_2). $B_1 = -\infty$ *or* $B_2 = +\infty$ *is allowed so that* $\widetilde{K}(x)$ *need not have compact support.*

(ii) $\widetilde{K}(x)$ *is continuous in* $\mathbb{R}$ *except possibly at* B_1, B_2, *where* $\lim_{x\to B_1^+}\widetilde{K}(x) = p_1$, $\lim_{x\to B_2^-}\widetilde{K}(x) = p_2$. *Also,* $\widetilde{K}(x)$ *may be written in the form*

$$\widetilde{K}(x) = \widetilde{K}_a(x) - p_1\chi_{(-\infty,B_1]} - p_2\chi_{[B_2,\infty)},$$

where $\widetilde{K}_a(x)$ *is absolutely continuous and* χ_S *is the indicator function of the set* S.

(iii) $\widetilde{K}(x)$ *is even and satisfies* $\int_{\mathbb{R}}\widetilde{K}(x)\mathbf{d}x = 1$.

(iv) $\widetilde{K}(x)$ is exponentially bounded, i.e., $\int_{\mathbb{R}} e^{\mu x}\widetilde{K}(x)\mathbf{d}x < +\infty$ for $\mu \neq 0$.

We are interested in two cases: $\Omega = \mathbb{R}$ and $\Omega = [-L, L]$, where L is a positive real number. For the former case, we study the relationship between the number of releasing infected males and the direction of traveling front, and for the latter, we investigate the critical patch size for persistence.

3.1. Traveling wave solutions to (3.1)

In this section, our aim is to discuss the traveling wave solutions of (3.1) in an unbounded domain. That is,

$$\omega_{t+1}(x) = \int_{-\infty}^{+\infty}\widetilde{K}(|x-y|)\Big[\frac{b\omega_t(y)}{1+R+\omega_t(y)}\frac{\omega_t(y)}{R+\omega_t(y)} + (1-d)\omega_t(y)\Big]\mathbf{d}y. \tag{3.2}$$

Based on the previous analysis, (1.6) admits three nonnegative equilibria if $b > d$, $0 < R < R^*$. It is a typical bistable structure where the equilibria satisfy $F'(0) < 1$, $F'(\omega_1^*) > 1$, and $F'(\omega_2^*) < 1$, respectively. To determine the direction of traveling wave solution, we introduce the following result.

Lemma 3.1. *[26] Assume that* $\widetilde{K}(|x-y|)$ *meets the conditions (i)–(iv), then there exists a unique nonincreasing traveling wave solution* $\omega_t(x) = W(x-st)$ *of* (3.2) *such that* $W(-\infty) = \omega_2^*$ *and* $W(+\infty) = 0$, *and* s *is the only spreading speed for which a nonincreasing traveling wave with value* ω_2^* *at* $-\infty$ *and* 0 *at* ∞ *can exist.*

The proof of Lemma 3.1 has already been guaranteed in Theorem 5 and Corollary 1 of [26], and details will not be repeated here. Now, according to Theorem 2.1 in [27], the direction of spreading speed s of traveling wave is determined by the sign of

$$\int_0^{\omega_2^*}(F(\omega)-\omega)\mathbf{d}\omega.$$

The following theorem deals with the issue proposed above.

Theorem 3.1. *Let* s *be the spreading speed for* (3.2). *Then there exists a threshold* $R^{**} \in (0, R^*)$ *such that the following statements hold.*

(i). $s > 0$ *if and only if* $R \in (0, R^{**})$;
(ii). $s = 0$ *if and only if* $R = R^{**}$;
(iii). $s < 0$ *if and only if* $R \in (R^{**}, R^*)$.

Proof. Let

$$G(R) = \int_0^{\omega_2^*(R)}(F(R,\omega)-\omega)\mathbf{d}\omega.$$

To prove Theorem 3.1, we first need to demonstrate that $G(R)$ is monotonically decreasing with R. Taking the derivative of $G(R)$ with respect to R yields

$$G'(R) = [F(\omega_2^*, R) - \omega_2^*]\frac{\mathbf{d}\omega_2^*}{\mathbf{d}R} + \int_0^{\omega_2^*(R)} \frac{\partial[F(R,\omega) - \omega]}{\partial R}\mathbf{d}\omega.$$

From (2.3), we have

$$F(\omega_2^*, R) - \omega_2^* = \left(\frac{b\omega_2^*}{(1 + R + \omega_2^*)(R + \omega_2^*)} - d\right)\omega_2^* = 0$$

and

$$\frac{\partial[F(R,\omega) - \omega]}{\partial R} = -\frac{b\omega^2(2R + 2\omega + 1)}{[(1 + R + \omega)(R + \omega)]^2} < 0.$$

Therefore, $G'(R) < 0$. Besides, we can calculate that

$$\begin{aligned} G(R) &= \int_0^{\omega_2^*}\left[\frac{b\omega}{1 + R + \omega}\frac{\omega}{R + \omega} - d\omega\right]\mathbf{d}\omega \\ &= \int_0^{\omega_2^*}\left[b\left(1 - \frac{(2R + 1)\omega + R(R + 1)}{(1 + R + \omega)(R + \omega)}\right) - d\omega\right]\mathbf{d}\omega \\ &= \int_0^{\omega_2^*}\left[b\left(1 + \frac{R^2}{\omega + R} - \frac{(R + 1)^2}{\omega + R + 1}\right) - d\omega\right]\mathbf{d}\omega \\ &= g(\omega_2^*) - g(0), \end{aligned} \tag{3.3}$$

where

$$g(\omega) = b(\omega + R^2\ln(\omega + R) - (R + 1)^2\ln(\omega + R + 1)) - \frac{d}{2}\omega^2. \tag{3.4}$$

Next, it follows from Lemma 2.2 that

$$\begin{aligned} \lim_{R\to 0} G(R) &= \lim_{R\to 0}\int_0^{\omega_2^*}(F(\omega) - \omega)\mathbf{d}\omega \\ &= \lim_{R\to 0}\left(g\left(\frac{b}{d} - 1\right) - g(0)\right) \\ &= b\left(\frac{b}{d} - \ln\frac{b}{d} - 1\right) - \frac{d}{2}\left(\frac{b}{d} - 1\right)^2. \end{aligned}$$

Let $\varphi = b\left(\frac{b}{d} - \ln\frac{b}{d} - 1\right) - \frac{d}{2}\left(\frac{b}{d} - 1\right)^2$ and $z = \frac{b}{d}$. From the condition $b > d$, we have $z > 1$ and

$$\frac{\varphi}{d} = z(z - \ln z - 1) - \frac{(z - 1)^2}{2} \triangleq m(z).$$

Differentiating $m(z)$ once, we get $m'(z) = z - \ln z - 1 > 0$ for any $z > 1$. Thus, $\lim_{z\to 1} m(z) = 0$ and $m(z) > 0$ for any $z > 1$, which implies $\lim_{R\to 0} G(R) > 0$. Similarly, we have

$$\begin{aligned} \lim_{R\to R^*} G(R) &= \int_0^{\frac{b^2 - d^2}{4bd}}(F(\omega) - \omega)\mathbf{d}\omega \\ &= g\left(\frac{b^2 - d^2}{4bd}\right) - g(0) < 0. \end{aligned}$$

Consequently, there exists a threshold $R^{**} \in (0, R^*)$ such that $G(R^{**}) = \int_0^{\omega_2^*}(F(\omega) - \omega)\mathbf{d}\omega = 0$, or equivalently, $s = 0$. If $R \in (0, R^{**})$, $G(R) = \int_0^{\omega_2^*}(F(\omega) - \omega)\mathbf{d}\omega > 0$, or equivalently, $s > 0$; if not, $s < 0$ when $R \in (R^{**}, R^*)$. Hence, the statements are proved.

3.2. Critical patch-size for the Laplace kernel in a bounded domain

In this section, we consider (3.1) with the interval $\Omega = [-L, L]$ and the Laplace kernel $\widetilde{K}(x - y) = \frac{a}{2}e^{-a|x-y|}$. Hence, (3.1) can be rewritten as

$$\omega_{t+1}(x) = \int_{-L}^{L} \frac{a}{2} e^{-a|x-y|}\left[\frac{b\omega_t(y)}{1 + R + \omega_t(y)}\frac{\omega_t(y)}{R + \omega_t(y)} + (1 - d)\omega_t(y)\right]\mathbf{d}y. \tag{3.5}$$

Clearly, (3.5) has a trivial equilibrium $\omega_0^*(x) = 0$. We will investigate the critical patch-size, denoted by L^*, for (3.5) in this section. If the patch is shorter than L^*, then dispersal loss exceeds reproductive gain in the patch, and the population will die out. If the patch is longer than L^*, then the situation is reversed, and the population can persist.

Let $\omega(x)$ be a positive equilibrium of (3.5), that is,

$$\begin{aligned}\omega(x) &= \int_{-L}^{L} \frac{a}{2} e^{-a|x-y|}\left[\frac{b\omega(y)}{1 + R + \omega(y)}\frac{\omega(y)}{R + \omega(y)} + (1 - d)\omega(y)\right]\mathbf{d}y\\ &= \frac{a}{2}\Bigg[\int_{-L}^{x} e^{-a(x-y)}\left(\frac{b\omega(y)}{1 + R + \omega(y)}\frac{\omega(y)}{R + \omega(y)} + (1 - d)\omega(y)\right)\mathbf{d}y\\ &\quad - \int_{L}^{x} e^{a(x-y)}\left(\frac{b\omega(y)}{1 + R + \omega(y)}\frac{\omega(y)}{R + \omega(y)} + (1 - d)\omega(y)\right)\mathbf{d}y\Bigg].\end{aligned} \tag{3.6}$$

By differentiating (3.6), we have

$$\begin{aligned}\omega'(x) = -\frac{a^2}{2}\Bigg[&\int_{-L}^{x} e^{-a(x-y)}\left(\frac{b\omega(y)}{1 + R + \omega(y)}\frac{\omega(y)}{R + \omega(y)} + (1 - d)\omega(y)\right)\mathbf{d}y\\ &+ \int_{L}^{x} e^{a(x-y)}\left(\frac{b\omega(y)}{1 + R + \omega(y)}\frac{\omega(y)}{R + \omega(y)} + (1 - d)\omega(y)\right)\mathbf{d}y\Bigg].\end{aligned} \tag{3.7}$$

Differentiating (3.7) again, we obtain

$$\begin{aligned}\omega''(x) \quad &= -a^2\left[\frac{b\omega(x)}{1 + R + \omega(x)}\frac{\omega(x)}{R + \omega(x)} + (1 - d)\omega(x)\right]\\ &\quad + \frac{a^3}{2}\int_{-L}^{L} e^{-a|x-y|}\left[\frac{b\omega(y)}{1 + R + \omega(y)}\frac{\omega(y)}{R + \omega(y)} + (1 - d)\omega(y)\right]\mathbf{d}y.\end{aligned} \tag{3.8}$$

Substituting (3.6) into (3.8) and rearranging the terms, we obtain the nonlinear differential equation

$$\omega'' = a^2\left[d\omega - \frac{b\omega}{1 + R + \omega}\frac{\omega}{R + \omega}\right], \quad x \in [-L, L]$$

with mixed boundary conditions

$$\omega'(-L) = a\omega(-L), \omega'(L) = -a\omega(L),$$

which are obtained by evaluating (3.7) at the boundary points. As a result, the existence of steady state for (3.5) is equivalent to the existence of equilibrium of a second-order differential equation with mixed boundary conditions.

Lemmas 4.1–4.3 in [28] and Theorem 3.1 indicate that if $R \in (0, R^{**})$, or equivalently, $\int_0^{\omega_2^*}(F(\omega) - \omega)\mathbf{d}\omega > 0$, then there exists a critical patch-size L^* for (3.5). Next, we will employ phase-plane methods to seek out the critical patch-size L^*. Now, suppose that $\widehat{\omega} = \omega'$. Then we have

$$\begin{cases} \frac{\mathbf{d}\omega}{\mathbf{d}x} = \widehat{\omega}, \\ \frac{\mathbf{d}\widehat{\omega}}{\mathbf{d}x} = a^2[d\omega - \frac{b\omega}{1+R+\omega}\frac{\omega}{R+\omega}], \\ \widehat{\omega}(-L) = a\omega(-L), \widehat{\omega}(L) = -a\omega(L). \end{cases} \tag{3.9}$$

Obviously, (3.9) has three steady states, $(0, 0)$, $(\omega_1^*, 0)$, and $(\omega_2^*, 0)$. It follows from (3.9) that

$$\frac{\mathbf{d}\widehat{\omega}}{\mathbf{d}\omega} = \frac{a^2[d\omega - \frac{b\omega}{1+R+\omega}\frac{\omega}{R+\omega}]}{\widehat{\omega}}. \tag{3.10}$$

Integrating both sides of (3.10) yields two solution trajectories on the plane $\omega - \widehat{\omega}$:

$$\begin{cases} S_0 : \widehat{\omega}^2 = 2a^2\int_0^{\omega}[d\nu - \frac{b\nu}{1+R+\nu}\frac{\nu}{R+\nu}]\mathbf{d}\nu = 2a^2(g(0) - g(\omega)), \quad \omega = 0 \Rightarrow \widehat{\omega} = 0, \\ S_1 : \widehat{\omega}^2 = 2a^2\int_{\omega}^{\omega_2^*}[\frac{b\nu}{1+R+\nu}\frac{\nu}{R+\nu} - d\nu]\mathbf{d}\nu = 2a^2(g(\omega_2^*) - g(\omega)), \quad \omega = \omega_2^* \Rightarrow \widehat{\omega} = 0, \end{cases} \tag{3.11}$$

where $g(\omega)$ is given by (3.4). Clearly, the curves S_0 and S_1 are symmetric about the horizontal axis of ω. From the Theorem 3.1, we obtain that if $R \in (0, R^{**})$, $\int_0^{\omega_2^*}(F(\omega)-\omega)\mathbf{d}\omega > 0$ and $\int_0^{\omega_1^*}(F(\omega)-\omega)\mathbf{d}\omega < 0$. Thus, there exists a positive value $p_0 \in (\omega_1^*, \omega_2^*)$ such that

$$\int_0^{p_0}(F(\nu) - \nu)\mathbf{d}\nu = 0.$$

For the case where $0 < \omega < p_0$, S_0 does not intersect with S_1; otherwise, there exists $\widetilde{\omega}$ satisfying $0 < \widetilde{\omega} < p_0$ such that $2a^2(g(0) - g(\widetilde{\omega})) = 2a^2(g(\omega_2^*) - g(\widetilde{\omega}))$. This implies that $g(\omega_2^*) - g(0) = 0$, which contradicts the fact that $g(\omega_2^*) - g(0) > 0$. Furthermore, from the expression of S_0, it is easy to see that

$$\widehat{\omega}^2 = 2a^2\int_0^{\omega}(\nu - F(\nu))\mathbf{d}\nu \le 2a^2\int_0^{\omega}\nu\mathbf{d}\nu = a^2\omega^2.$$

This inequality shows that S_0 is located between the boundary lines of $\widehat{\omega} = a\omega$ and $\widehat{\omega} = -a\omega$.

The trajectory S_1 has a point intersecting with the boundary condition $\widehat{\omega} = a\omega$ due to $\widehat{\omega}^2 = 2a^2(g(\omega_2^*) - g(0)) > 0$. Denote the intersecting point as $\overline{q}$. Then $\overline{q}$ satisfies

$$\omega^2 = 2(g(\omega_2^*) - g(\omega)). \tag{3.12}$$

For every $q \in (0, \overline{q})$, the trajectory (noted as S) starting at (q, aq) and located between S_0 and S_1 corresponds to the equilibrium $\omega(x)$ of (3.9). Integrating both sides of (3.10) with ω ranging from q to ω and $\widehat{\omega}$ ranging from aq to $\widehat{\omega}$, S is given by

$$\widehat{\omega}^2 = 2a^2\int_q^{\omega}(\nu - F(\nu))\mathbf{d}\nu + a^2q^2 = 2a^2[g(q) - g(\omega)] + a^2q^2. \tag{3.13}$$

Let $p(q)$ be the intersection point of trajectory S and the ω horizontal axis, as shown in Figure 3. Then $\omega = p(q)$ satisfies the following equation:

$$2[g(q) - g(\omega)] + q^2 = 0.$$

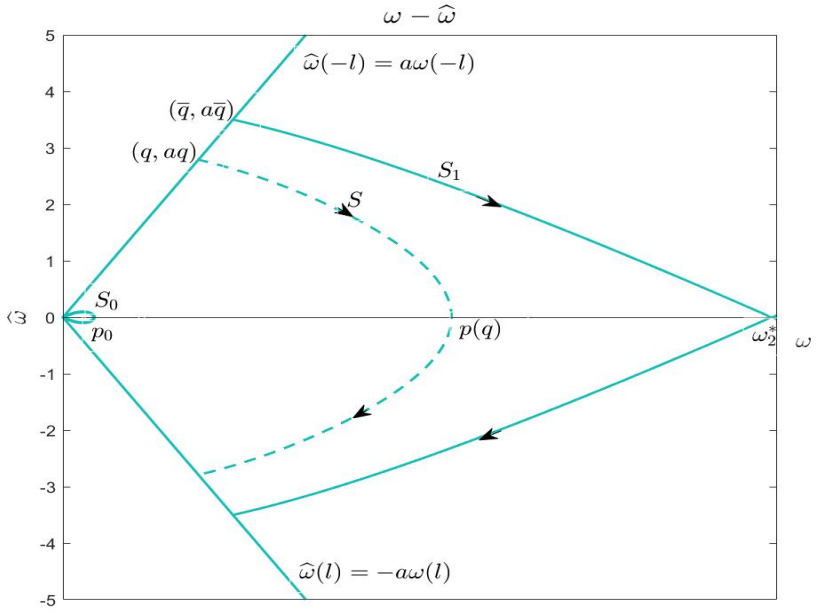

Figure 3. Analysis of $\omega - \widehat{\omega}$ phase plane. S_0, S_1, and S are the trajectories for (3.11) and (3.13), respectively. p_0, ω_2^*, and $p(q)$ are, respectively, the intersection points of the trajectories S_0, S_1, and S with the ω-axis.

Combining (3.12) and the first equation of (3.9), we have

$$\frac{\mathbf{d}\omega}{\mathbf{d}x} = a\sqrt{2[g(q) - g(\omega)] + q^2}. \tag{3.14}$$

If $q < \omega < p(q)$, $-L < x < 0$, then integrating (3.14) leads to

$$L(q) = \int_q^{p(q)} \frac{1}{a\sqrt{2[g(q) - g(\omega)] + q^2}} \mathbf{d}\omega. \tag{3.15}$$

Here, L is defined as a function of q for $0 < q < \overline{q}$.

To establish our claim that (3.5) admits a critical patch-size, we now proceed to sequentially verify the properties of $L(q)$. As $q \to \overline{q}$, $p(q) \to \omega_2^*$. It follows from (3.15) that

$$\lim_{q\to\overline{q}} L(q) = \int_{\overline{q}}^{\omega_2^*} \frac{1}{a\sqrt{2[g(\overline{q}) - g(\omega)] + \overline{q}^2}} \mathbf{d}\omega.$$

Take $f(\omega) = 2[g(\overline{q}) - g(\omega)] + \overline{q}^2$ and expand $f(\omega)$ around $\omega = \omega_2^*$:

$$f(\omega) = f(\omega_2^*) + \frac{\partial f(\omega_2^*)}{\partial \omega}(\omega - \omega_2^*) + \frac{1}{2!}\frac{\partial^2 f(\omega_2^*)}{\partial \omega^2}(\omega - \omega_2^*)^2 + \dots .$$

Furthermore, the definition of $\overline{q}$ indicates that $f(\omega_2^*) = 0$ and $f'(\omega_2^*) = -2g'(\omega_2^*) = 0$, from which the order of zero of $f(\omega)$ for $\omega = \omega_2^*$ is at least 2, and consequently, as $q \to \overline{q}$, $L(q) \to \infty$. So, the similar conclusion that $\lim_{q\to 0} = \infty$ can be obtained.

Arguing as before, it can be concluded that minimum patch-size

$$L^* = \inf_{0<q<\overline{q}} \int_q^{p(q)} \frac{1}{a\sqrt{2[g(q) - g(\omega)] + q^2}} \mathbf{d}\omega, \tag{3.16}$$

is always well defined, and there are at least two different corresponding values for q in (3.14) when $L > L^*$. This implies that (3.5) admits at least two positive equilibria, and we denote the largest one as $\omega^*(x)$.

Now, we have the following theorem regarding the positive steady $\omega^*(x)$.

Theorem 3.2. *The following statements hold:*

i. Suppose that $R \in (0, R^{**})$. Then (3.5) *has a critical patch-size L^* such that:*

(a) If $L > L^*$, there exists a positive steady state $\omega^*(x)$ for (3.5) *such that if $\omega^*(x) \le \omega_0(x) \le \omega_2^*$, then*

$$\lim_{t\to\infty} \omega_t(x) = \omega^*(x), \quad x \in [-L, L];$$

(b) If $L < L^*$, there is no positive steady state, and the solution $\omega_t(x)$ of (3.5) *with $0 \le \omega_0(x) \le \omega_2^*$ has a property that*

$$\lim_{t\to\infty} \omega_t(x) = 0, \quad x \in [-L, L];$$

ii. Suppose that $R \in (R^{**}, R^*)$. Then for any L, there is no positive steady state for (3.5)*, and in this case, for $0 \le \omega_0(x) \le \omega_2^*$, we have*

$$\lim_{t\to\infty} \omega_t(x) = 0, \quad x \in [-L, L].$$

Proof. (i) If $R \in (0, R^{**})$, then from the previous discussion, we get $\int_0^{\omega_2^*}(F(\omega) - \omega)\mathbf{d}\omega > 0$ and a critical patch-size L^* as shown in (3.16). By applying Theorem 4.1 in [28], the result is easy to obtain.

(ii) A similar proof process can also lead to this result.

4. Numerical simulation

To numerically validate the results of (1.6), we set the following parameter values: $b = 4$, $c = 1$, and $d = 0.2$. So, $r^* = \frac{(b-d)^2}{4bcd} = 4.5125$ can be derived from (2.2).

In Case(i), wild mosquito population is unaffected by infected males. Figure 4(A) shows that the number of wild mosquito population will eventually converge to the globally asymptotically stable state $\omega_1^* = 19$ for any initial value.

If wild mosquito population is affected by the *Wolbachia*-infected males and the complete CI effect occurs, the system exhibits complex dynamical behavior. In Case(ii), numerical simulations demonstrate that (1.6) admits three equilibria, $\omega_0^* = 0$, $\omega_1^* \approx 0.4113$, and $\omega_2^* \approx 14.5888$, when $r = 2 \in (0, r^*)$. As illustrated in Figure 4(B), the system displays a bistable structure with a critical initial value threshold at ω_1^*, above which (1.6) has an asymptotically stable positive equilibrium ω_2^* and below which (1.6) has a locally asymptotically stable zero equilibrium point. This result implies that when the initial population of wild mosquito is relatively small, releasing a small number of infected male mosquitoes can also successfully suppress them. In Case(iii), when $r = r^* = 4.5125$, the system exhibits two equilibria, $\omega_0^* = 0$ and $\omega^* = 4.9875$. Figure 4(C) illustrates the corresponding wild mosquito population trajectory ω_t, demonstrating the local asymptotic stability of both equilibria. Similar to Case(iv), the population dynamics depend critically on the initial wild mosquito population. If the release number $r = 6 \in (r^*, +\infty) > r^*$, (1.6) has a globally asymptotically extinction state $\omega_0^* = 0$; see Figure 4(D). The biological meaning of this is that whatever the initial value of wild mosquito population is, it will eventually be suppressed by infected males if the release value r is large enough.

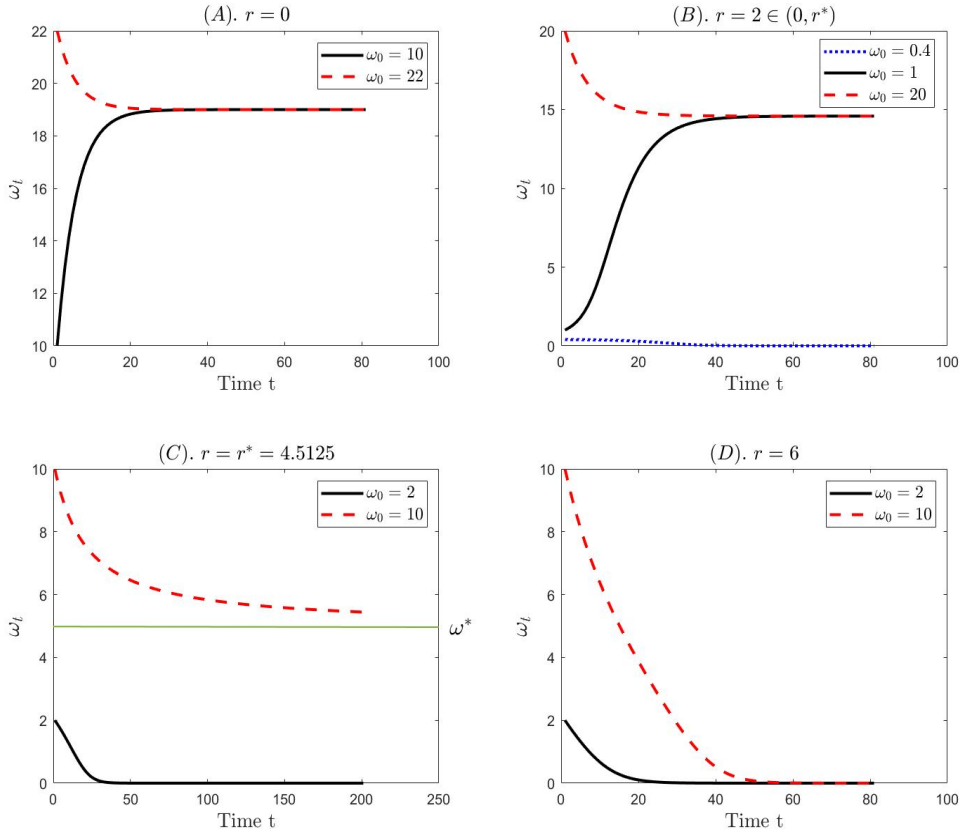

Figure 4. $(A) - (D)$ show the variation of ω_t under four different conditions of $Case(i) - (iv)$.

As for (3.5), we conduct numerical simulations by using the Laplace kernel $\widetilde{K}(x)$ with $a = 1$ and the

growth function $F(x)$ with $b = 4$, $c = 1$, and $d = 0.2$. According to Theorem 3.1, we obtain the critical release threshold $r^{**} = R^{**} \approx 4.2697$. When $r \in (0, 4.2697)$, it has $\int_0^{\omega_2^*}(F(\omega) - \omega)\mathbf{d}\omega > 0$. By selecting $r = 2 \in (0, r^{**})$, we depict L with respect to q in Figure 5 based on Eq (3.15). In this case, the critical patch-size $L^* \approx 0.1954$. If the habitat patch of wild mosquito population L exceeds $L^* \approx 0.1954$, Theorem 3.2 asserts that (3.5) has a positive equilibrium, which implies that the suppression of infected males fails. If not, the mosquito population suppression is successful.

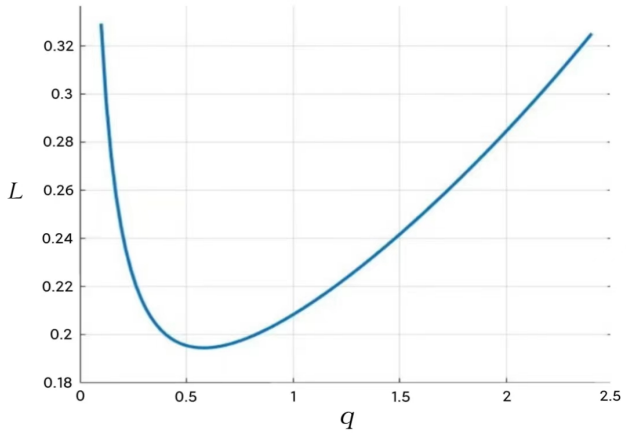

Figure 5. q-L as determined by (3.15).

5. Concluding remarks

In this paper, we formulate an overlapping generation discrete model for the mosquito population suppression. Under different release strategies, we have derived the threshold value r^* for the releasing of infected males. If r is greater than, equal to, or less than r^*, there may be zero, one, or two positive equilibria in (1.6). It also means whether the wild mosquito population can be successfully suppressed or not. By applying bifurcation theory, we have demonstrated that (1.6) undergoes a saddle-node bifurcation at $r = r^*$. At last, if the birth rate b increases or the competition coefficient c decreases, the releasing threshold r^* will become larger. That is, more infected males need to be released to inhibit the growth of wild mosquito population.

However, different from the previous discrete model, we also formulate an integro-difference equation to predict the dynamics of wild mosquito population in both an unbounded and bounded habitat patch. The results of the spatial model have shown that if the habitat patch of wild mosquito population is considered as a one-dimensional unbounded domain, i.e., $\Omega = (-\infty, +\infty)$, then there exists a nonincreasing traveling wave solution $\omega_t(x) = W(x - st)$ with a spreading speed c such that $W(-\infty) = \omega_2^*$ and $W(+\infty) = 0$. The speed of the traveling wave solution is related to the number of infected males. We can prove that (3.2) possesses a threshold value $r^{**} \in (0, r^*)$, which determines the direction of traveling waves. For $r \in (0, r^{**})$, (3.2) has a traveling wave solution moving rightward, and for $r \in (r^{**}, r^*)$, it has a traveling wave solution moving leftward. As for the bounded habitat

patch $\Omega = [-L, L]$, if the number of infected males $r \in (0, r^{**})$, then (3.5) admits a critical patch-size L^*, above which a locally attracting positive equilibrium $\omega^*(x)$ emerges for a suitable choice of initial distribution and the *Wolbachia* invasion fails, and below which all the solution converges to zero and the *Wolbachia* invasion is guaranteed to be successful. If $r^{**} < r < r^*$, then all solutions of (3.5) tend to zero for all $L > 0$. In contrast to the difference equation model, our analysis reveals two key findings. One is that diffusion is beneficial to reduce the release threshold value of the infected males in mosquito population suppression. The other is that if the release quantity of infected males is less than r^{**}, the habitat of wild mosquito population needs to remain below the critical patch size L^* for the successful suppression.

Use of AI tools declaration

The authors declare they have not used Artificial Intelligence (AI) tools in the creation of this article.

Acknowledgments

This project is supported by the National Natural Science Foundation of China(No. 12571193 and 12171110), the Science and Technology Planning Project of Guangzhou, China (2024A03J0381) and the Graduate Innovation Ability Training Project of Guangzhou University (JCCX2024-015).

Conflict of interest

The authors declare there are no conflicts of interest.

References

1. J. C. Semenza, J. E. Suk, Vector-borne diseases and climate change: a European perspective, *FEMS Microbiol. Lett.*, **365** (2018), fnx244. https://doi.org/10.1093/femsle/fnx244
2. P. E. Simonsen, M. E. Mwakitalu, Urban lymphatic filariasis, *Parasitol. Res.*, **112** (2013), 35–44. https://doi.org/10.1007/s00436-012-3226-x
3. F. G. Sauer, E. Kiel, R. Lühken, Effects of mosquito resting site temperatures on the estimation of pathogen development rates in near-natural habitats in Germany, *Parasites Vectors*, **15** (2022), 390. https://doi.org/10.1186/s13071-022-05505-2
4. J. Kronen, M. Leuchner, T. Küpper, Zika and chikungunya in Europe 2100-a GIS based model for risk estimation, *Travel Med. Infect. Dis.*, **60** (2024), 102737. https://doi.org/10.1016/j.tmaid.2024.102737
5. M. B. Thomas, Biological control of human disease vectors: a perspective on challenges and opportunities, *BioControl*, **63** (2018), 61–69. https://doi.org/10.1007/s10526-017-9815-y
6. H. A. Flores, S. L. O'Neill, Controlling vector-borne diseases by releasing modified mosquitoes, *Nat. Rev. Microbiol.*, **16** (2018), 508–518. https://doi.org/10.1038/s41579-018-0025-0
7. I. Iturbe-Ormaetxe, T. Walker, S. L. O'Neill, Wolbachia and the biological control of mosquito-borne disease, *EMBO Rep.*, **12** (2011), 508–518. https://doi:10.1038/embor.2011.84

8. J. H. Yen, A. R. Barr, New hypothesis of the cause of cytoplasmic incompatibility in culex pipiens L., *Nature*, **232** (1971), 657–658. https://doi.org/10.1038/232657a0
9. X. Zheng, D. Zhang, Y. Li, C. Yang, Y. Wu, X. Liang, et al., Incompatible and sterile insect techniques combined eliminate mosquitoes, *Nature*, **572** (2019), 56–61. https://doi.org/10.1038/s41586-019-1407-9
10. Y. Li, L. A. Baton, D. Zhang, J. Bouyer, A. G. Parker, A. A. Hoffmann, et al., Reply to: Issues with combining incompatible and sterile insect techniques, *Nature*, **590** (2021), E3–E5. https://doi.org/10.1038/s41586-020-03165-9
11. Z. Zhang, L. Chang, Q. Huang, R. Yan, B. Zheng, A mosquito population suppression model with a saturated Wolbachia release strategy in seasonal succession, *J. Math. Biol.*, **86** (2023), 51. https://doi.org/10.1007/s00285-023-01888-7
12. B. Zheng, J. Yu, At most two periodic solutions for a switching mosquito population suppression model, *J. Dyn. Differ. Equations*, **35** (2023), 2997–3009. https://doi.org/10.1007/s10884-021-10125-y
13. Y. Li , X. Liu, A sex-structured model with birth pulse and release strategy for the spread of Wolbachia in mosquito population, *J. Theor. Biol.*, **448** (2018), 53–65. https://doi.org/10.1016/j.jtbi.2018.04.001
14. R. Jiang, Z. Guo, Dynamics of discrete Ricker models on mosquito population suppression, *Math. Methods Appl. Sci.*, **47** (2024), 4821–4839. https://doi.org/10.1002/mma.9840
15. B. Zheng, J. Yu, Existence and uniqueness of periodic orbits in a discrete model on Wolbachia infection frequency, *Adv. Nonlinear Anal.*, **11** (2022), 212–224. https://doi.org/10.1515/anona-2020-0194
16. J. Yu, J. Li, Discrete-time models for interactive wild and sterile mosquitoes with general time steps, *Math. Biosci.*, **346** (2022), 108797. https://doi.org/10.1016/j.mbs.2022.108797
17. Y. Li, J. Li, Discrete-time models for releases of sterile mosquitoes with Beverton-Holt-type of survivability, *Ric. Mat.*, **67** (2018), 141–162. https://doi.org/10.1007/s11587-018-0361-4
18. Q. Chen, Z. Teng, F. Wang, Fold-flip and strong resonance bifurcations of a discrete-time mosquito model, *Chaos, Solitons Fractals*, **144** (2021), 110704. https://doi.org/10.1016/j.chaos.2021.110704
19. Y. Liu, Z. Guo, M. S. El, L. Wang, A Wolbachia infection model with free boundary, *J. Biol. Dyn.*, **14** (2020), 515–542. https://doi.org/10.1080/17513758.2020.1784474
20. K. Wang, H. Wang, H. Zhao, On the role of advection in a spatial epidemic model with general boundary conditions, *J. Differ. Equations*, **386** (2024), 45–79. https://doi.org/10.1016/j.jde.2023.12.016
21. K. Wang, H. Wang, H. Zhao, Global threshold dynamics of a spatial chemotactic mosquito-borne disease model, *IMA J. Appl. Math.*, **88** (2023), 354–377. https://doi.org/10.1093/imamat/hxad009
22. J. Yu, J. Li, Discrete-time models for interactive wild and transgenic sterile mosquitoes, *J. Differ. Equations Appl.*, **30** (2024), 1590–1609. https://doi.org/10.1080/10236198.2024.2325485
23. R. J. H. Beverton, S. J. Holt, *On the Dynamics of Exploited Fish Populations*, 1st edition, Springer Netherlands, London, 2012. https://doi.org/10.1007/978-94-011-2106-4

24. D. Zhang, R. S. Lees, Z. Xi, J. R. L. Gilles, K. Bourtzis, Combining the sterile insect technique with Wolbachia-based approaches: II-a safer approach to *Aedes albopictus* population suppression programmes, designed to minimize the consequences of inadvertent female release, *PLoS One*, **10** (2015), e0135194. https://doi.org/10.1371/journal.pone.0135194

25. F. Lutscher, *Integrodifference Equations in Spatial Ecology*, 1st edition, Springer, Cham, 2019. https://doi.org/10.1007/978-3-030-29294-2

26. R. Lui, Existence and stability of travelling wave solutions of a nonlinear integral operator, *J. Math. Biol.*, **16** (1983), 199–220. https://doi.org/10.1007/BF00276502

27. M. H. Wang, M. Kot, M. G. Neubert, Integrodifference equations, Allee effects, and invasions, *J. Math. Biol.*, **44** (2002), 150–168. https://doi.org/10.1007/s002850100116

28. B. Li, G. Otto, Wave speed and critical patch size for integro-difference equations with a strong Allee effect, *J. Math. Biol.*, **85** (2022), 59. https://doi.org/10.1007/s00285-022-01814-3

AIMS Press